PROCEEDINGS OF THE ROYAL SOCIETY A

Proc. R. Soc. A (2006) **462**, 3629–3643
doi:10.1098/rspa.2006.1742
Published online 27 June 2006

Steering laws for motion camouflage

By E. W. Justh[1] and P. S. Krishnaprasad[1,2,*]

[1]*Institute for Systems Research, and* [2]*Department of Electrical and Computer Engineering, University of Maryland, College Park, MD 20742, USA*

Motion camouflage is a stealth strategy observed in nature. We formulate the problem as a feedback system for particles moving at constant speed, and define what it means for the system to be in a state of motion camouflage. (Here, we focus on the planar setting, although the results can be generalized to three-dimensional motion.) We propose a biologically plausible feedback law, and use a high-gain limit to prove the accessibility of a motion-camouflage state in finite time. We discuss connections to work in missile guidance. We also present simulation results to explore the performance of the motion-camouflage feedback law for a variety of settings.

Keywords: motion camouflage; missile guidance; proportional navigation

1. Introduction

Motion camouflage is a stealth strategy employed by various visual insects and animals to achieve prey capture, mating or territorial combat. In one type of motion camouflage, the predator camouflages itself against a fixed background object so that the prey observes no relative motion between the predator and the fixed object. In the other type of motion camouflage, the predator approaches the prey such that from the point of view of the prey, the predator always appears to be at the same bearing. (In this case, we say that the object against which the predator is camouflaged is a point at infinity.) The motion-camouflage strategy serves to minimize *motion parallax* cues that moving prey would be able to extract from the apparent relative motion of objects at various distances (Srinivasan & Davey 1995). For example, insects with compound eyes are quite sensitive to optical flow (which arises from the transverse component of the relative velocity between the predator and the prey), but are far less sensitive to looming (which arises from the component of the relative velocity between the predator and the prey along the line joining them). More broadly, such interactions may also apply to settings of mating activity or territorial manoeuvre as well. In Srinivasan & Davey (1995), it was suggested that the data on visually mediated interactions between two hoverflies *Syritta pipiens*, obtained earlier by Collett & Land (1975), support a motion-camouflage hypothesis. Later, Mizutani *et al.* (2003), observing the territorial aerial manoeuvres of dragonflies *Hemianax papuensis*, concluded that the flight pattern is motivated by motion camouflage (see fig. 1 in Mizutani *et al.* 2003). See also Srinivasan & Zhang (2004) for a review of related themes in insect vision and flight control.

* Author for correspondence (krishna@umd.edu).

Received 12 January 2006
Accepted 11 May 2006

Motion camouflage can be used by a predator to stealthily pursue the prey, but a motion-camouflage strategy can also be used by the prey to evade a predator. The only difference between the strategy of the predator and the strategy of the evader is that the predator seeks to approach the prey while maintaining motion camouflage, whereas the evader seeks to move away from the predator while maintaining motion camouflage. Besides explaining certain biological pursuit strategies, motion camouflage may also be quite useful in certain military scenarios (although the 'predator' and 'prey' labels may not be descriptive). In some settings, as is the case in Collett & Land (1975), Srinivasan & Davey (1995) and Mizutani *et al.* (2003), it is more appropriate to substitute the labels 'shadower' and 'shadowee' for the predator–prey terminology.

The essential geometry of motion camouflage (see §2*a*) is not limited to encounters between visual insects. In a recent work on the neuroethology of insect-capture behaviour in echolocating bats, a strategy geometrically indistinguishable from motion camouflage is observed (Ghose *et al.* 2006).

In this work, we take a structured approach to derive feedback laws for motion camouflage, which incorporates biologically plausible (vision) sensor measurements. We model the predator and prey as point particles moving at constant (but different) speeds, and subject to steering (curvature) control. For an appropriate choice of feedback control law for one of the particles (as the other follows a prescribed trajectory), a state of motion camouflage is then approached as the system evolves. (In the situation where the predator follows a motion-camouflage law, and the speed of the predator exceeds the speed of the prey, the predator is able to pass 'close' to the prey in finite time. In practice, once the predator is sufficiently close to the prey, it would change its strategy from a pursuit strategy to an intercept strategy.)

What distinguishes this work from an earlier study on motion-camouflage trajectories in Glendinning (2004) is that we present *biologically plausible feedback laws* leading to motion camouflage. Furthermore, unlike the neural-network approach used in Anderson & McOwan (2003*a*) to achieve motion camouflage using biologically plausible sensor data, our approach gives an explicit form for the feedback law which has a straightforward physical interpretation.

The study of motion-camouflage problems also naturally extends earlier work on interacting systems of particles, using the language of curves and moving frames (Justh & Krishnaprasad 2002, 2003, 2005; Zhang *et al.* 2004).

2. Planar pursuit–evasion model

For concreteness, we consider the problem of motion camouflage in which the predator (which we refer to as the 'pursuer') attempts to intercept the prey (which we refer to as the 'evader') while it appears to the prey as if it is always at the same bearing (i.e. motion camouflaged against a point at infinity). In this model, we consider that the pursuer moves at unit speed in the plane, while the evader moves at a constant speed $\nu<1$. The dynamics of the pursuer are given by

$$\left.\begin{aligned}\dot{\boldsymbol{r}}_{\mathrm{p}} &= \boldsymbol{x}_{\mathrm{p}},\\ \dot{\boldsymbol{x}}_{\mathrm{p}} &= \boldsymbol{y}_{\mathrm{p}} u_{\mathrm{p}},\\ \dot{\boldsymbol{y}}_{\mathrm{p}} &= -\boldsymbol{x}_{\mathrm{p}} u_{\mathrm{p}},\end{aligned}\right\} \tag{2.1}$$

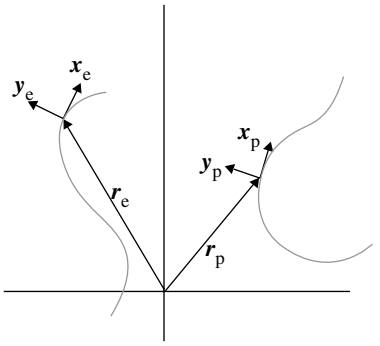

Figure 1. Planar trajectories for the pursuer and evader, and their respective natural Frenet frames.

where $\boldsymbol{r}_p$ is the position of the pursuer, $\boldsymbol{x}_p$ is the unit tangent vector to the trajectory of the pursuer, $\boldsymbol{y}_p$ is the corresponding unit normal vector (which completes a right-handed orthonormal basis with $\boldsymbol{x}_p$), and the plane curvature u_p is the steering control for the pursuer. Similarly, the dynamics of the evader are

$$\left.\begin{aligned} \dot{\boldsymbol{r}}_e &= \nu \boldsymbol{x}_e, \\ \dot{\boldsymbol{x}}_e &= \nu \boldsymbol{y}_e u_e, \\ \dot{\boldsymbol{y}}_e &= -\nu \boldsymbol{x}_e u_e, \end{aligned}\right\} \tag{2.2}$$

where $\boldsymbol{r}_e$ is the position of the evader, $\boldsymbol{x}_e$ is the unit tangent vector to the trajectory of the evader, $\boldsymbol{y}_e$ is the corresponding unit normal vector and u_e is the steering control for the evader. Figure 1 illustrates equations (2.1) and (2.2). Note that $\{\boldsymbol{x}_p, \boldsymbol{y}_p\}$ and $\{\boldsymbol{x}_e, \boldsymbol{y}_e\}$ are planar natural Frenet frames for the trajectories of the pursuer and evader, respectively.

We model the pursuer and evader as point particles (confined to the plane), and use natural frames and curvature controls to describe their motion, because this is a simple model for which we can derive both physical intuition and concrete control laws. (Furthermore, this approach generalizes nicely for three-dimensional motion, as in Justh & Krishnaprasad (2005) and Reddy *et al.* (2006).) Flying insects and animals (also unmanned aerial vehicles) have limited manoeuvrability and must maintain sufficient airspeed to stay aloft, so that treating their motion as constant speed with steering control is physically reasonable, at least for some range of flight conditions. (Note that the steering control directly drives the angular velocity of the particle, and hence is actually an acceleration input. However, this acceleration is constrained to be perpendicular to the instantaneous direction of motion, and therefore, the speed remains unchanged.)

We refer to (2.1) and (2.2) as the 'pursuit–evader system'. In what follows, we assume that the pursuer follows a *feedback* strategy to drive the system towards a state of motion camouflage, and close in on the evader. The evader, on the other hand, follows an open-loop strategy. The analysis we present for the pursuer feedback strategy also suggests (with a sign change in the control law) how the evader could use feedback and a motion-camouflage strategy to conceal its flight from the pursuer. Ultimately, it would be interesting to investigate the game-theoretic problem in which both the pursuer and the evader follow feedback strategies, so that the system would truly be a pursuit–evader system. (What we address in this work would be more properly described as a pursuer–pursuee

system. However, we keep the pursuer–evader terminology because it sets the stage for analysing the true pursuer–evader system, which we aim to discuss in a future paper.)

Equations (2.1) and (2.2) represent curve evolution for two particles in the Lie group $SE(2)$ of rigid motions in the plane. In the setting of cooperative interacting particles, generalization to the three-dimensional setting is developed in Justh & Krishnaprasad (2005).

(*a*) *Motion camouflage with respect to a point at infinity*

Motion camouflage with respect to a point at infinity is given by

$$\boldsymbol{r}_{\mathrm{p}} = \boldsymbol{r}_{\mathrm{e}} + \lambda \boldsymbol{r}_{\infty}, \tag{2.3}$$

where $\boldsymbol{r}_{\infty}$ is a fixed unit vector and λ is a time-dependent scalar (see also §5 in Glendinning (2004)). In the rest of this paper, it should be understood that by 'motion camouflage' we mean *with respect to a point at infinity* (see, however, §6).

Let

$$\boldsymbol{r} = \boldsymbol{r}_{\mathrm{p}} - \boldsymbol{r}_{\mathrm{e}}, \tag{2.4}$$

be the vector from the evader to the pursuer. We refer to $\boldsymbol{r}$ as the 'baseline vector', and $|\boldsymbol{r}|$ as the 'baseline length'. We restrict our attention to non-collision states, i.e. $\boldsymbol{r} \neq 0$. In that case, the component of the pursuer velocity $\dot{\boldsymbol{r}}_{\mathrm{p}}$ transverse to the base line is

$$\dot{\boldsymbol{r}}_{\mathrm{p}} - \left(\frac{\boldsymbol{r}}{|\boldsymbol{r}|} \cdot \dot{\boldsymbol{r}}_{\mathrm{p}}\right) \frac{\boldsymbol{r}}{|\boldsymbol{r}|},$$

and similarly, that of the evader is

$$\dot{\boldsymbol{r}}_{\mathrm{e}} - \left(\frac{\boldsymbol{r}}{|\boldsymbol{r}|} \cdot \dot{\boldsymbol{r}}_{\mathrm{e}}\right) \frac{\boldsymbol{r}}{|\boldsymbol{r}|}.$$

The *relative* transverse component is

$$\boldsymbol{w} = (\dot{\boldsymbol{r}}_{\mathrm{p}} - \dot{\boldsymbol{r}}_{\mathrm{e}}) - \left(\frac{\boldsymbol{r}}{|\boldsymbol{r}|} \cdot (\dot{\boldsymbol{r}}_{\mathrm{p}} - \dot{\boldsymbol{r}}_{\mathrm{e}})\right) \frac{\boldsymbol{r}}{|\boldsymbol{r}|} \quad = \dot{\boldsymbol{r}} - \left(\frac{\boldsymbol{r}}{|\boldsymbol{r}|} \cdot \dot{\boldsymbol{r}}\right) \frac{\boldsymbol{r}}{|\boldsymbol{r}|}. \tag{2.5}$$

Lemma 2.1 Infinitesimal characterization of motion camouflage. *The pursuit–evasion system (2.1)–(2.2) is in a state of motion camouflage without collision on an interval iff* $\boldsymbol{w} = 0$ *on that interval.*

Proof. ($\Rightarrow$) Suppose motion camouflage holds. Thus,

$$\boldsymbol{r}(t) = \lambda(t)\boldsymbol{r}_{\infty}, \quad t \in [0, T]. \tag{2.6}$$

Differentiating, $\dot{\boldsymbol{r}} = \dot{\lambda}\boldsymbol{r}_{\infty}$. Hence, noting that $|\lambda| \neq 0$ under non-collision,

$$\boldsymbol{w} = \dot{\boldsymbol{r}} - \left(\frac{\boldsymbol{r}}{|\boldsymbol{r}|} \cdot \dot{\boldsymbol{r}}\right) \frac{\boldsymbol{r}}{|\boldsymbol{r}|} = \dot{\lambda}\boldsymbol{r}_{\infty} - \left(\frac{\lambda}{|\lambda|}\boldsymbol{r}_{\infty} \cdot \dot{\lambda}\boldsymbol{r}_{\infty}\right) \frac{\lambda}{|\lambda|}\boldsymbol{r}_{\infty} = 0 \ \text{ on } [0, T]. \tag{2.7}$$

($\Leftarrow$) Suppose $\boldsymbol{w} = 0$ on $[0, T]$. Thus,

$$\dot{\boldsymbol{r}} = \left(\frac{\boldsymbol{r}}{|\boldsymbol{r}|} \cdot \dot{\boldsymbol{r}}\right) \frac{\boldsymbol{r}}{|\boldsymbol{r}|} \triangleq \xi \boldsymbol{r}, \tag{2.8}$$

so that

$$\boldsymbol{r}(t) = \exp\left(\int_0^t \xi(\sigma)\mathrm{d}\sigma\right)\boldsymbol{r}(0) = |\boldsymbol{r}(0)|\exp\left(\int_0^t \xi(\sigma)\mathrm{d}\sigma\right)\frac{\boldsymbol{r}(0)}{|\boldsymbol{r}(0)|} = \lambda(t)\boldsymbol{r}_\infty, \tag{2.9}$$

where $\boldsymbol{r}_\infty = \boldsymbol{r}(0)/|\boldsymbol{r}(0)|$ and $\lambda(t) = |\boldsymbol{r}(0)|\exp(\int_0^t \xi(\sigma)\mathrm{d}\sigma)$. ■

It follows from lemma 2.1 that the set of all motion-camouflage states constitutes a five-dimensional smooth manifold with two connected components (one corresponding to approach and the other corresponding to retreat), each diffeomorphic to $S^1 \times \mathbb{R} \times SE(2)$ in the six-dimensional state space $SE(2) \times SE(2)$ of the problem. In practice, we are interested in knowing how far is the pursuit–evasion system from a state of motion camouflage. In what follows, we offer a measure of this.

(*b*) *Cost function*

Consider the ratio

$$\Gamma(t) = \frac{\frac{\mathrm{d}}{\mathrm{d}t}|\boldsymbol{r}|}{\left|\frac{\mathrm{d}\boldsymbol{r}}{\mathrm{d}t}\right|}, \tag{2.10}$$

which compares the rate of change of the baseline length to the absolute rate of change of the baseline vector. If the baseline experiences pure lengthening, then the ratio assumes its maximum value, $\Gamma(t) = 1$. If the baseline experiences pure shortening, then the ratio assumes its minimum value, $\Gamma(t) = -1$. If the baseline experiences pure rotation, but remains of the same length, then $\Gamma(t) = 0$. Noting that

$$\frac{\mathrm{d}}{\mathrm{d}t}|\boldsymbol{r}| = \frac{\boldsymbol{r}}{|\boldsymbol{r}|}\cdot\dot{\boldsymbol{r}}, \tag{2.11}$$

we see that $\Gamma(t)$ may alternatively be written as

$$\Gamma(t) = \left(\frac{\boldsymbol{r}}{|\boldsymbol{r}|}\cdot\frac{\dot{\boldsymbol{r}}}{|\dot{\boldsymbol{r}}|}\right). \tag{2.12}$$

Thus, $\Gamma(t)$ is the dot product of two unit vectors: one in the direction of $\boldsymbol{r}$, and the other in the direction of $\dot{\boldsymbol{r}}$. Note that Γ is well defined except at $\boldsymbol{r} = 0$, since

$$1 - \nu \le |\dot{\boldsymbol{r}}| = |\boldsymbol{x}_\mathrm{p} - \nu\boldsymbol{x}_\mathrm{e}| \le 1 + \nu. \tag{2.13}$$

For convenience, we define the notation $\boldsymbol{q}^\perp$ to represent the vector $\boldsymbol{q}$ rotated counter-clockwise in the plane by an angle $\pi/2$. Thus, for example, $\boldsymbol{x}_\mathrm{p}^\perp = \boldsymbol{y}_\mathrm{p}$. The transverse component $\boldsymbol{w}$ of relative velocity, expression (2.5), then becomes

$$\boldsymbol{w} = \dot{\boldsymbol{r}} - \left(\frac{\boldsymbol{r}}{|\boldsymbol{r}|}\cdot\dot{\boldsymbol{r}}\right)\frac{\boldsymbol{r}}{|\boldsymbol{r}|} = \left[\left(\frac{\boldsymbol{r}}{|\boldsymbol{r}|}\right)^\perp\cdot\dot{\boldsymbol{r}}\right]\left(\frac{\boldsymbol{r}}{|\boldsymbol{r}|}\right)^\perp = -\left(\frac{\boldsymbol{r}}{|\boldsymbol{r}|}\cdot\dot{\boldsymbol{r}}^\perp\right)\left(\frac{\boldsymbol{r}}{|\boldsymbol{r}|}\right)^\perp. \tag{2.14}$$

For convenience, we define w to be the (signed) magnitude of $\boldsymbol{w}$, i.e.

$$w = \boldsymbol{w}\cdot\left(\frac{\boldsymbol{r}}{|\boldsymbol{r}|}\right)^\perp = -\left(\frac{\boldsymbol{r}}{|\boldsymbol{r}|}\cdot\dot{\boldsymbol{r}}^\perp\right), \tag{2.15}$$

and refer also to w as the transverse component of the relative velocity. From the orthogonal decomposition

$$\frac{\boldsymbol{r}}{|\boldsymbol{r}|} = \left(\frac{\boldsymbol{r}}{|\boldsymbol{r}|}\cdot\frac{\dot{\boldsymbol{r}}}{|\dot{\boldsymbol{r}}|}\right)\left(\frac{\dot{\boldsymbol{r}}}{|\dot{\boldsymbol{r}}|}\right) + \left[\frac{\boldsymbol{r}}{|\boldsymbol{r}|}\cdot\left(\frac{\dot{\boldsymbol{r}}}{|\dot{\boldsymbol{r}}|}\right)^{\perp}\right]\left(\frac{\dot{\boldsymbol{r}}}{|\dot{\boldsymbol{r}}|}\right)^{\perp}, \tag{2.16}$$

it follows that

$$1 = \left(\frac{\boldsymbol{r}}{|\boldsymbol{r}|}\cdot\frac{\dot{\boldsymbol{r}}}{|\dot{\boldsymbol{r}}|}\right)^2 + \left[\frac{\boldsymbol{r}}{|\boldsymbol{r}|}\cdot\left(\frac{\dot{\boldsymbol{r}}}{|\dot{\boldsymbol{r}}|}\right)^{\perp}\right]^2 = \Gamma^2 + \frac{|w|^2}{|\dot{\boldsymbol{r}}|^2}. \tag{2.17}$$

Thus, $(1-\Gamma^2)$ is a measure of departure from motion camouflage.

(*c*) *Feedback law derivation*

Differentiating Γ along trajectories of (2.1) and (2.2) gives

$$\begin{aligned}\dot{\Gamma} &= \left(\frac{\dot{\boldsymbol{r}}\cdot\dot{\boldsymbol{r}}+\boldsymbol{r}\cdot\ddot{\boldsymbol{r}}}{|\boldsymbol{r}||\dot{\boldsymbol{r}}|}\right) - \left(\frac{\boldsymbol{r}\cdot\dot{\boldsymbol{r}}}{|\dot{\boldsymbol{r}}|}\right)\left(\frac{\boldsymbol{r}\cdot\dot{\boldsymbol{r}}}{|\boldsymbol{r}|^3}\right) - \left(\frac{\boldsymbol{r}\cdot\dot{\boldsymbol{r}}}{|\boldsymbol{r}|}\right)\left(\frac{\boldsymbol{r}\cdot\ddot{\boldsymbol{r}}}{|\dot{\boldsymbol{r}}|^3}\right)\\ &= \frac{|\dot{\boldsymbol{r}}|}{|\boldsymbol{r}|}\left[1-\left(\frac{\boldsymbol{r}}{|\boldsymbol{r}|}\cdot\frac{\dot{\boldsymbol{r}}}{|\dot{\boldsymbol{r}}|}\right)^2\right] + \frac{1}{|\dot{\boldsymbol{r}}|}\left[\frac{\boldsymbol{r}}{|\boldsymbol{r}|} - \left(\frac{\boldsymbol{r}}{|\boldsymbol{r}|}\cdot\frac{\dot{\boldsymbol{r}}}{|\dot{\boldsymbol{r}}|}\right)\frac{\dot{\boldsymbol{r}}}{|\dot{\boldsymbol{r}}|}\right]\cdot\ddot{\boldsymbol{r}}.\end{aligned} \tag{2.18}$$

From (2.4) we obtain

$$\dot{\boldsymbol{r}}^{\perp} = \boldsymbol{y}_{\mathrm{p}} - \nu\boldsymbol{y}_{\mathrm{e}}, \tag{2.19}$$

and

$$\ddot{\boldsymbol{r}} = \boldsymbol{y}_{\mathrm{p}}u_{\mathrm{p}} - \nu^2\boldsymbol{y}_{\mathrm{e}}u_{\mathrm{e}}. \tag{2.20}$$

Also,

$$\left[\frac{\boldsymbol{r}}{|\boldsymbol{r}|} - \left(\frac{\boldsymbol{r}}{|\boldsymbol{r}|}\cdot\frac{\dot{\boldsymbol{r}}}{|\dot{\boldsymbol{r}}|}\right)\frac{\dot{\boldsymbol{r}}}{|\dot{\boldsymbol{r}}|}\right] = \left[\frac{\boldsymbol{r}}{|\boldsymbol{r}|}\cdot\left(\frac{\dot{\boldsymbol{r}}}{|\dot{\boldsymbol{r}}|}\right)^{\perp}\right]\left(\frac{\dot{\boldsymbol{r}}}{|\dot{\boldsymbol{r}}|}\right)^{\perp} = \frac{1}{|\dot{\boldsymbol{r}}|^2}\left(\frac{\boldsymbol{r}}{|\boldsymbol{r}|}\cdot\dot{\boldsymbol{r}}^{\perp}\right)\dot{\boldsymbol{r}}^{\perp}. \tag{2.21}$$

Then, from (2.18), we obtain

$$\begin{aligned}\dot{\Gamma} &= \frac{|\dot{\boldsymbol{r}}|}{|\boldsymbol{r}|}\left[1-\left(\frac{\boldsymbol{r}}{|\boldsymbol{r}|}\cdot\frac{\dot{\boldsymbol{r}}}{|\dot{\boldsymbol{r}}|}\right)^2\right] + \frac{1}{|\dot{\boldsymbol{r}}|}\left[\frac{\boldsymbol{r}}{|\boldsymbol{r}|} - \left(\frac{\boldsymbol{r}}{|\boldsymbol{r}|}\cdot\frac{\dot{\boldsymbol{r}}}{|\dot{\boldsymbol{r}}|}\right)\frac{\dot{\boldsymbol{r}}}{|\dot{\boldsymbol{r}}|}\right]\cdot(\boldsymbol{y}_{\mathrm{p}}u_{\mathrm{p}} - \nu^2\boldsymbol{y}_{\mathrm{e}}u_{\mathrm{e}})\\ &= \frac{|\dot{\boldsymbol{r}}|}{|\boldsymbol{r}|}\left[\frac{1}{|\dot{\boldsymbol{r}}|^2}\left(\frac{\boldsymbol{r}}{|\boldsymbol{r}|}\cdot\dot{\boldsymbol{r}}^{\perp}\right)^2\right] + \frac{1}{|\dot{\boldsymbol{r}}|}\left[\frac{1}{|\dot{\boldsymbol{r}}|^2}\left(\frac{\boldsymbol{r}}{|\boldsymbol{r}|}\cdot\dot{\boldsymbol{r}}^{\perp}\right)\dot{\boldsymbol{r}}^{\perp}\right]\cdot(\boldsymbol{y}_{\mathrm{p}}u_{\mathrm{p}} - \nu^2\boldsymbol{y}_{\mathrm{e}}u_{\mathrm{e}}).\end{aligned} \tag{2.22}$$

Noting that

$$\dot{\boldsymbol{r}}^{\perp}\cdot\boldsymbol{y}_{\mathrm{p}} = \dot{\boldsymbol{r}}\cdot\boldsymbol{x}_{\mathrm{p}} = 1-\nu(\boldsymbol{x}_{\mathrm{p}}\cdot\boldsymbol{x}_{\mathrm{e}}) \geq 1-\nu > 0, \tag{2.23}$$

and

$$\dot{\boldsymbol{r}}^{\perp}\cdot\boldsymbol{y}_{\mathrm{e}} = \dot{\boldsymbol{r}}\cdot\boldsymbol{x}_{\mathrm{e}} = (\boldsymbol{x}_{\mathrm{p}}\cdot\boldsymbol{x}_{\mathrm{e}}) - \nu, \tag{2.24}$$

we obtain

$$\dot{I} = \frac{|\dot{\boldsymbol{r}}|}{|\boldsymbol{r}|}\left[\frac{1}{|\dot{\boldsymbol{r}}|^2}\left(\frac{\boldsymbol{r}}{|\boldsymbol{r}|}\cdot\dot{\boldsymbol{r}}^{\perp}\right)^2\right] + \frac{1}{|\dot{\boldsymbol{r}}|}\left[\frac{1}{|\dot{\boldsymbol{r}}|^2}\left(\frac{\boldsymbol{r}}{|\boldsymbol{r}|}\cdot\dot{\boldsymbol{r}}^{\perp}\right)\right](1-\nu(\boldsymbol{x}_{\mathrm{p}}\cdot\boldsymbol{x}_{\mathrm{e}}))u_{\mathrm{p}}$$
$$+\frac{1}{|\dot{\boldsymbol{r}}|}\left[\frac{1}{|\dot{\boldsymbol{r}}|^2}\left(\frac{\boldsymbol{r}}{|\boldsymbol{r}|}\cdot\dot{\boldsymbol{r}}^{\perp}\right)\right](\nu-(\boldsymbol{x}_{\mathrm{p}}\cdot\boldsymbol{x}_{\mathrm{e}}))\nu^2 u_{\mathrm{e}}. \tag{2.25}$$

Suppose that we take

$$u_{\mathrm{p}} = -\mu\left(\frac{\boldsymbol{r}}{|\boldsymbol{r}|}\cdot\dot{\boldsymbol{r}}^{\perp}\right) + \left[\frac{(\boldsymbol{x}_{\mathrm{p}}\cdot\boldsymbol{x}_{\mathrm{e}})-\nu}{1-\nu(\boldsymbol{x}_{\mathrm{p}}\cdot\boldsymbol{x}_{\mathrm{e}})}\right]\nu^2 u_{\mathrm{e}}, \tag{2.26}$$

where $\mu>0$, so that the steering control for the pursuer consists of two terms: one involving the motion of the evader, and the other involving the transverse component of the relative velocity. Then,

$$\dot{I} = -\left[\frac{\mu}{|\dot{\boldsymbol{r}}|}(1-\nu(\boldsymbol{x}_{\mathrm{p}}\cdot\boldsymbol{x}_{\mathrm{e}}))-\frac{|\dot{\boldsymbol{r}}|}{|\boldsymbol{r}|}\right]\left[\frac{1}{|\dot{\boldsymbol{r}}|}\left(\frac{\boldsymbol{r}}{|\boldsymbol{r}|}\cdot\dot{\boldsymbol{r}}^{\perp}\right)\right]^2, \tag{2.27}$$

and for any choice of $\mu>0$, there exists $r_{\mathrm{o}}>0$ such that

$$\frac{\mu}{|\dot{\boldsymbol{r}}|}(1-\nu(\boldsymbol{x}_{\mathrm{p}}\cdot\boldsymbol{x}_{\mathrm{e}}))-\frac{|\dot{\boldsymbol{r}}|}{|\boldsymbol{r}|}>0, \tag{2.28}$$

for all $\boldsymbol{r}$ such that $|\boldsymbol{r}|>r_{\mathrm{o}}$. Thus, for control law (2.26),

$$\dot{I}\leq 0, \quad \forall|\boldsymbol{r}|>r_{\mathrm{o}}. \tag{2.29}$$

3. The high-gain limit

Control law (2.26) has the nice property that for any value of the gain $\mu>0$, there is a disc of radius r_{o} (depending on μ) such that $\dot{I}\leq 0$ outside the disc. However, the problem with (2.26) is that the pursuer needs to know (i.e. sense and estimate) the evader's steering programme u_{e}. Here we show that by taking μ as sufficiently large, motion camouflage can be achieved (in a sense we will make precise) using a control law depending only on the transverse relative velocity,

$$u_{\mathrm{p}} = -\mu\left(\frac{\boldsymbol{r}}{|\boldsymbol{r}|}\cdot\dot{\boldsymbol{r}}^{\perp}\right), \tag{3.1}$$

in place of (2.26), provided $|u_{\mathrm{e}}|$ is bounded. Comparing (3.1) to (2.15), we see that, indeed, u_{p} is proportional to the signed length of the relative transverse velocity vector. We will designate this as the *motion camouflage proportional guidance* (MCPG) law for future reference (see §5).

As is further discussed in §5, (3.1) requires range information as well as pure optical flow sensing. However, the range information can be coarse since range errors (within appropriate bounds) have the same effect in (3.1) as gain variations. We say that (3.1) is *biologically plausible* because the only critical sensor measurement required is optical flow sensing. Optical flow sensing does not yield the relative transverse velocity directly, but rather the angular speed of the image

of the evader across the pursuer's eye. In fact, it is the sign of the optical flow that is most critical to measure correctly, since errors in the magnitude of the optical flow, like range errors, only serve to modulate the gain in (3.1).

For biological systems, the capabilities of the sensors *vis-à-vis* the sensing requirements for implementing (3.1) constrain the range of conditions for which (3.1) represents a feasible control strategy. In the high-gain limit we focus on below, the sensor noise (which is amplified by the high gain) would be expected to have significant impact. However, to illustrate the essential behaviour, here we neglect both sensor limitations and noise.

(*a*) *Bounds and estimates*

Let us consider control law (3.1), and the resulting behaviour of Γ as a function of time. From (2.25), we obtain the inequality

$$\begin{aligned}
\dot{\Gamma} &= -\left[\frac{\mu}{|\dot{\boldsymbol{r}}|}(1-\nu(\boldsymbol{x}_{\mathrm{p}}\cdot\boldsymbol{x}_{\mathrm{e}}))-\frac{|\dot{\boldsymbol{r}}|}{|\boldsymbol{r}|}\right]\left[\frac{1}{|\dot{\boldsymbol{r}}|}\left(\frac{\boldsymbol{r}}{|\boldsymbol{r}|}\cdot\dot{\boldsymbol{r}}^{\perp}\right)\right]^{2}\\
&\quad+\frac{1}{|\dot{\boldsymbol{r}}|}\left[\frac{1}{|\dot{\boldsymbol{r}}|^{2}}\left(\frac{\boldsymbol{r}}{|\boldsymbol{r}|}\cdot\dot{\boldsymbol{r}}^{\perp}\right)\right](\nu-(\boldsymbol{x}_{\mathrm{p}}\cdot\boldsymbol{x}_{\mathrm{e}}))\nu^{2}u_{\mathrm{e}}\\
&\leq -(1-\Gamma^{2})\left[\frac{\mu}{|\dot{\boldsymbol{r}}|}(1-\nu(\boldsymbol{x}_{\mathrm{p}}\cdot\boldsymbol{x}_{\mathrm{e}}))-\frac{|\dot{\boldsymbol{r}}|}{|\boldsymbol{r}|}\right]+\frac{1}{|\dot{\boldsymbol{r}}|^{2}}\sqrt{1-\Gamma^{2}}|(\nu-(\boldsymbol{x}_{\mathrm{p}}\cdot\boldsymbol{x}_{\mathrm{e}}))\nu^{2}u_{\mathrm{e}}|\\
&\leq -(1-\Gamma^{2})\left[\frac{\mu}{|\dot{\boldsymbol{r}}|}(1-\nu)-\frac{|\dot{\boldsymbol{r}}|}{|\boldsymbol{r}|}\right]+(\sqrt{1-\Gamma^{2}})\frac{\nu^{2}(1+\nu)(\max|u_{\mathrm{e}}|)}{|\dot{\boldsymbol{r}}|^{2}}\\
&\leq -(1-\Gamma^{2})\left[\mu\left(\frac{1-\nu}{1+\nu}\right)-\frac{1+\nu}{|\boldsymbol{r}|}\right]+(\sqrt{1-\Gamma^{2}})\left[\frac{\nu^{2}(1+\nu)(\max|u_{\mathrm{e}}|)}{(1-\nu)^{2}}\right],
\end{aligned}\tag{3.2}$$

where we have used (2.13). For convenience, we define the constant $c_1>0$ as

$$c_1=\frac{\nu^{2}(1+\nu)(\max|u_{\mathrm{e}}|)}{(1-\nu)^{2}}.\tag{3.3}$$

For any $\mu>0$, we can define $r_{\mathrm{o}}>0$ and $c_{\mathrm{o}}>0$ such that

$$\mu=\left(\frac{1+\nu}{1-\nu}\right)\left(\frac{1+\nu}{r_{\mathrm{o}}}+c_{\mathrm{o}}\right),\tag{3.4}$$

(and it is clear that many such choices of r_{o} and c_{o} exist). Note that (3.4) implies

$$\mu\geq\left(\frac{1+\nu}{1-\nu}\right)\left(\frac{1+\nu}{|\boldsymbol{r}|}+c_{\mathrm{o}}\right),\quad\forall|\boldsymbol{r}|\geq r_{\mathrm{o}}.\tag{3.5}$$

Thus, for $|\boldsymbol{r}|\geq r_{\mathrm{o}}$, (3.2) becomes

$$\begin{aligned}
\dot{\Gamma}&\leq -(1-\Gamma^{2})\left[\left(\frac{1+\nu}{1-\nu}\right)\left(\frac{1+\nu}{|\boldsymbol{r}|}+c_{\mathrm{o}}\right)\left(\frac{1-\nu}{1+\nu}\right)-\frac{1+\nu}{|\boldsymbol{r}|}\right]+(\sqrt{1-\Gamma^{2}})c_1\\
&=-(1-\Gamma^{2})c_{\mathrm{o}}+(\sqrt{1-\Gamma^{2}})c_1.
\end{aligned}\tag{3.6}$$

Suppose that given $0<\epsilon\ll 1$, we take $c_{\mathrm{o}}\geq 2c_1/\sqrt{\epsilon}$. Then, for $(1-\Gamma^2)>\epsilon$,

$$\dot{\Gamma}\leq -(1-\Gamma^2)c_{\mathrm{o}}+(\sqrt{1-\Gamma^2})c_1=-(1-\Gamma^2)\left(c_{\mathrm{o}}-\frac{c_1}{\sqrt{1-\Gamma^2}}\right)$$

$$\leq -(1-\Gamma^2)\left(c_{\mathrm{o}}-\frac{c_1}{\sqrt{\epsilon}}\right)=-(1-\Gamma^2)c_2, \tag{3.7}$$

where

$$c_2=c_{\mathrm{o}}-\frac{c_1}{\sqrt{\epsilon}}>0. \tag{3.8}$$

Remark 3.1. There are two possibilities for

$$(1-\Gamma^2)\leq\epsilon. \tag{3.9}$$

The state we seek to drive the system toward has $\Gamma\approx -1$; however, (3.9) can also be satisfied for $\Gamma\approx 1$. (Recall that $-1\leq\Gamma\leq 1$.) There is always a set of initial conditions such that (3.9) is satisfied with $\Gamma\approx 1$. We can address this issue as follows: let $\epsilon_{\mathrm{o}}>0$ denote how close to -1 we wish to drive Γ, and let $\Gamma_0=\Gamma(0)$ denote the initial value of Γ. Take

$$\epsilon=\min(\epsilon_{\mathrm{o}},1-\Gamma_0^2), \tag{3.10}$$

so that (3.7) with (3.8) applies from time $t=0$.

From (3.7), we can write

$$\frac{\mathrm{d}\Gamma}{1-\Gamma^2}\leq -c_2\mathrm{d}t, \tag{3.11}$$

which, on integrating both sides, leads to

$$\int_{\Gamma_0}^{\Gamma}\frac{\mathrm{d}\tilde{\Gamma}}{1-\tilde{\Gamma}^2}\leq -c_2\int_0^t\mathrm{d}\tilde{t}=-c_2t, \tag{3.12}$$

where $\Gamma_0=\Gamma(t=0)$. Noting that

$$\int_{\Gamma_0}^{\Gamma}\frac{\mathrm{d}\tilde{\Gamma}}{1-\tilde{\Gamma}^2}=\int_{\Gamma_0}^{\Gamma}\mathrm{d}(\tanh^{-1}\tilde{\Gamma})=\tanh^{-1}\Gamma-\tanh^{-1}\Gamma_0, \tag{3.13}$$

we see that for $|\boldsymbol{r}|\geq r_{\mathrm{o}}$, (3.7) implies

$$\Gamma(t)\leq\tanh(\tanh^{-1}\Gamma_0-c_2t), \tag{3.14}$$

where we have used the fact that $\tanh^{-1}(\cdot)$ is a monotone increasing function.

Now we consider estimating how long $|\boldsymbol{r}|\geq r_{\mathrm{o}}$, which in turn determines how large t can become in inequality (3.14), and hence how close to -1 will $\Gamma(t)$ be driven. From (2.12), we have

$$\frac{\mathrm{d}}{\mathrm{d}t}|\boldsymbol{r}|=\Gamma(t)|\dot{\boldsymbol{r}}|, \tag{3.15}$$

which from (2.13) and $|\Gamma(t)|\leq 1$, $\forall t$, implies

$$\frac{\mathrm{d}}{\mathrm{d}t}|\boldsymbol{r}|\geq -|\Gamma(t)|(1+\nu)\geq -(1+\nu). \tag{3.16}$$

From (3.16), we conclude that

$$|\boldsymbol{r}(t)| \geq |\boldsymbol{r}(0)| - (1+\nu)t, \quad \forall t \geq 0, \tag{3.17}$$

and, more to the point,

$$|\boldsymbol{r}(t)| \geq r_{\mathrm{o}}, \quad \forall t \leq \frac{|\boldsymbol{r}(0)| - r_{\mathrm{o}}}{1+\nu}. \tag{3.18}$$

For (3.18) to be meaningful for the problem at hand, we assume that $|\boldsymbol{r}(0)| > r_{\mathrm{o}}$. Then, defining

$$T = \frac{|\boldsymbol{r}(0)| - r_{\mathrm{o}}}{1+\nu} > 0, \tag{3.19}$$

to be the minimum interval of time over which we can guarantee that $\dot{\Gamma} \leq 0$, we conclude that

$$\Gamma(T) \leq \tanh(\tanh^{-1}\Gamma_0 - c_2 T). \tag{3.20}$$

From (3.20), we see that by choosing c_2 to be sufficiently large (which can be accomplished by choosing $c_{\mathrm{o}} \geq 2c_1/\sqrt{\epsilon}$ to be sufficiently large), we can force $\Gamma(T) \leq -1+\epsilon$. Noting that

$$\tanh(x) \leq -1+\epsilon \Leftrightarrow x \leq \frac{1}{2}\ln\Big(\frac{\epsilon}{2-\epsilon}\Big), \tag{3.21}$$

for $0 < \epsilon \ll 1$, we see that

$$\Gamma(T) \leq -1+\epsilon \Leftarrow \tanh^{-1}\Gamma_0 - c_2 T \leq \frac{1}{2}\ln\Big(\frac{\epsilon}{2-\epsilon}\Big). \tag{3.22}$$

Thus, if $c_{\mathrm{o}} \geq 2c_1/\sqrt{\epsilon}$ is taken to be sufficiently large such that

$$c_2 \geq (1+\nu)\frac{\tanh^{-1}\Gamma_0 - \frac{1}{2}\ln\left(\frac{\epsilon}{2-\epsilon}\right)}{|\boldsymbol{r}(0)| - r_{\mathrm{o}}}, \tag{3.23}$$

then we are guaranteed (under the conditions mentioned in the above calculations) to achieve $\Gamma(t_1) \leq -1+\epsilon$ at some finite time $t_1 \leq T$.

(*b*) *Statement of result*

Definition 3.2. Given the system (2.1)–(2.2) with Γ defined by (2.12), we say that 'motion camouflage is accessible in finite time' if for any $\epsilon > 0$ there exists a time $t_1 > 0$ such that $\Gamma(t_1) \leq -1+\epsilon$.

Proposition 3.3. *Consider the system (2.1)–(2.2) with Γ defined by (2.12), and control law (3.1), with the following hypotheses:*

(A1) $0 < \nu < 1$ *(and ν is constant),*
(A2) u_{e} *is continuous and* $|u_{\mathrm{e}}|$ *is bounded,*
(A3) $\Gamma_0 = \Gamma(0) < 1$, *and*
(A4) $|\boldsymbol{r}(0)| > 0$.

Motion camouflage is accessible in finite time using high-gain feedback (i.e. by choosing $\mu > 0$ sufficiently large).

Proof. Choose $r_o > 0$ such that $r_o < |\boldsymbol{r}(0)|$. Choose $c_2 > 0$ sufficiently large so as to satisfy (3.23), and choose c_o accordingly to ensure that (3.7) holds for $\Gamma > -1 + \epsilon$. Then, defining μ according to (3.4) ensures that $\Gamma(T) \leq -1 + \epsilon$, where $T > 0$ is defined by (3.19). ■

Remark 3.4. Assumption (A 1) can be generalized to $0 \leq \nu < 1$. (The case $\nu = 0$ corresponds to a stationary 'evader', so that the natural Frenet frame (2.2) and steering control u_e for the evader are not defined.)

4. Simulation results

The following simulation results illustrate the behaviour of the pursuit–evasion system (2.1)–(2.2), under the control law (3.1) for the pursuer and various open-loop controls for the evader. The simulations also confirm the analytical results presented earlier. Figure 2 shows the behaviour of the system for the simplest evader behaviour, $u_e = 0$, which corresponds to straight-line motion. Because control law (3.1) is the same as (2.26) when $u_e = 0$, Γ tends monotonically towards -1 (for the initial conditions and choice of gain μ used in the simulation shown). In figure 2, as in the subsequent figures showing pursuer and evader trajectories, the solid light lines connect the pursuer and evader positions at evenly spaced time instants. For a pursuit–evasion system in a state of motion camouflage, these lines would all be parallel to one another. Also, each simulation is run for a finite time, at the end of which the pursuer and evader are in close proximity. (The ratio of speeds is $\nu = 0.9$ in all the simulations shown.)

Figure 3 illustrates the behaviour of the pursuer for a sinsusoidally varying steering control u_e of the evader, and the corresponding behaviour of $\Gamma(t)$. Increase in the value of the feedback gain μ by a factor of three is observed to decrease the peak difference between Γ and -1 by a factor of about $3^2 = 9$. This is consistent with the calculations in the proof of proposition 3.3. Figure 4 illustrates the behaviour of the pursuer for a randomly varying steering control u_e of the evader, as well as the corresponding behaviour of $\Gamma(t)$. Similar to figure 3, figure 4 shows that increase in the feedback gain μ by a factor of three decreases the peak difference between Γ and -1 by a factor of about $3^2 = 9$. Figure 4 also shows the value of initial transient in $\Gamma(t)$ for t as small. As would be expected, increase in the gain μ increases the convergence rate. Figure 5 suggests a graceful degradation in performance in the presence of sensor noise—a key requirement for biological plausibility.

5. Connections to missile guidance

There is a vast literature on the subject of missile guidance in which the problem of pursuit of a (evasively) manoeuvring target by a tactical missile is of central interest. A particular class of feedback laws, known as *pure proportional navigation guidance* (PPNG) occupies a prominent place (Shneydor 1998). For planar missile–target engagements, the PPNG law determining the steering control for the missile/pursuer is

$$u^{\mathrm{PPNG}} = N\dot{\lambda}, \tag{5.1}$$

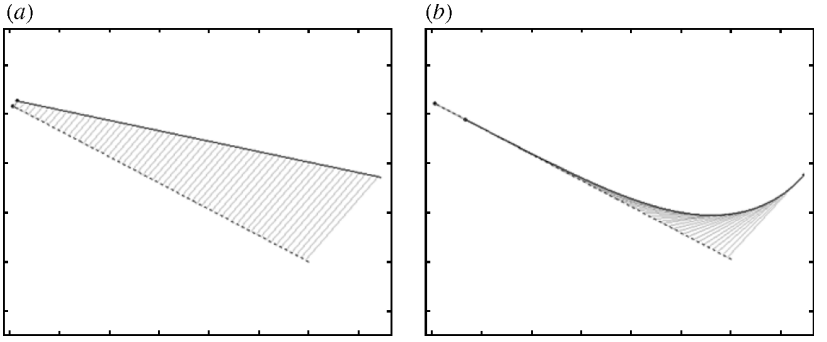

Figure 2. (*a*) Straight-line evader trajectory (dashed dark line), and the corresponding pursuer trajectory (solid dark line) evolving according to (2.1) with control given by (3.1). (*b*) An alternative pursuit law based on following a direct bearing towards the evader, shown for the same duration of time and the same initial conditions as in (*a*). Because strategy (3.1) is time optimal, while the direct-bearing law is not, the direct-bearing law requires longer time to achieve the same separation tolerance (about 1.7 times as long in this simulation). For the evader following a straight-line path, both the motion camouflage and classic pursuit (i.e. direct-bearing) strategies can be integrated explicitly and compared as in Glendinning (2004).

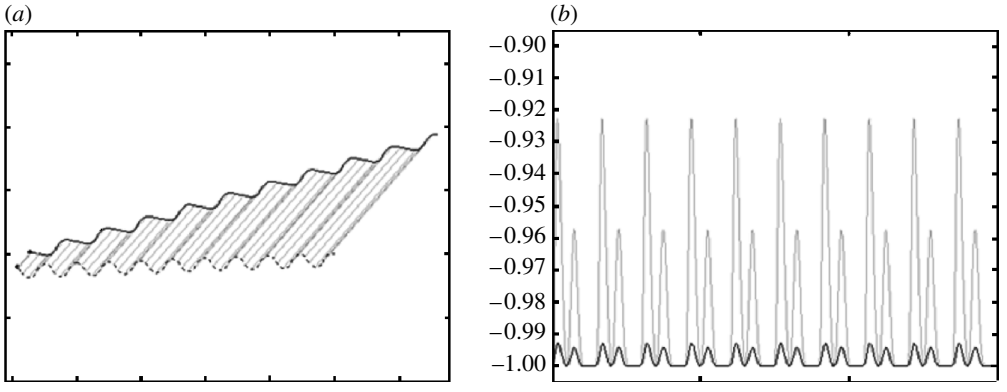

Figure 3. (*a*) Evader trajectory with sinusoidally varying steering input (dashed dark line), and the corresponding pursuer trajectory (solid dark line) evolving according to (2.1) with control given by (3.1). (*b*) The corresponding cost function $\Gamma(t)$ given by (2.12), plotted as a function of time. The two traces correspond to different values of gain μ: the value of μ is three times as large for the dark trace as for the light trace. (The trajectories corresponding to the two different gains are qualitatively similar; (*a*) actually corresponds to the lower value of μ.).

where $\dot{\lambda}$ denotes the rate of rotation (in the plane) of the line-of-sight vector from the pursuer to the evader (not to be confused with the λ in §2*a*). Here the gain N is a dimensionless positive constant known as the navigation constant. Note that our motion camouflage proportional guidance (MCPG) law given by (3.1) has a gain μ, which has the dimensions of $[\mathrm{LENGTH}]^{-1}$. Also, it is easy to see that

$$\dot{\lambda} = \frac{w}{|\boldsymbol{r}|} = -\frac{1}{|\boldsymbol{r}|}\left(\frac{\boldsymbol{r}}{|\boldsymbol{r}|}\cdot\dot{\boldsymbol{r}}^{\perp}\right). \tag{5.2}$$

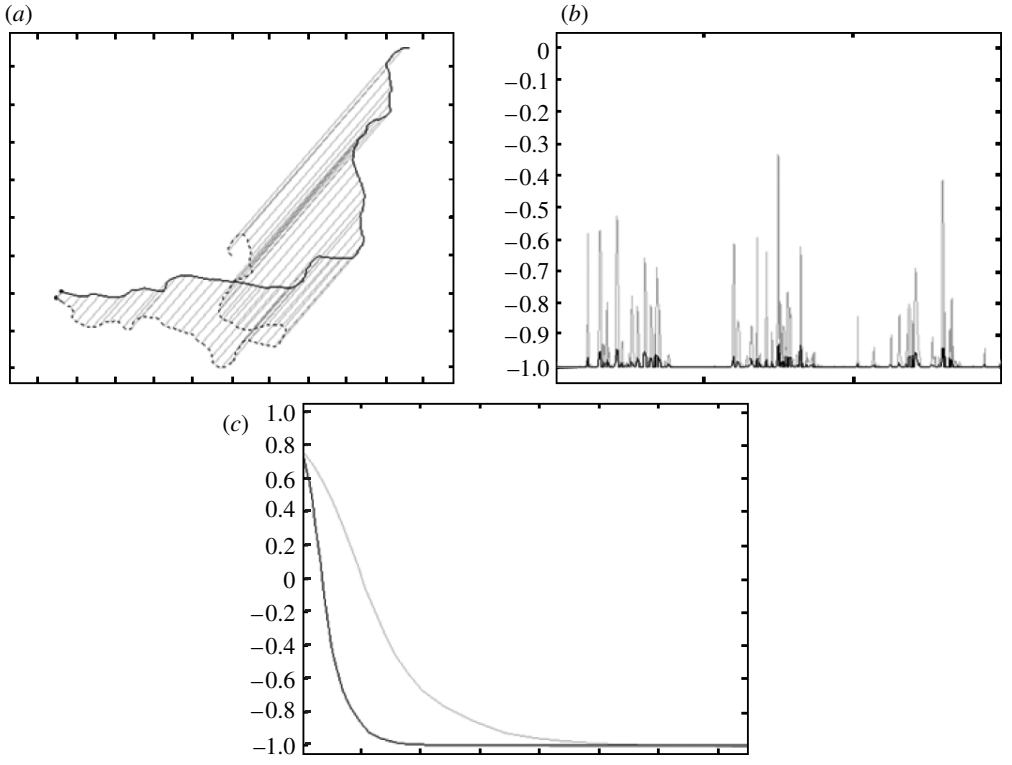

Figure 4. (*a*) Evader trajectory with randomly varying steering input (dashed dark line), and the corresponding pursuer trajectory (solid dark line) evolving according to (2.1) with control given by (3.1). (*b*) The corresponding cost function $\Gamma(t)$ given by (2.12), plotted as a function of time. The two traces correspond to different values of gain μ: the value of μ is three times as large for the dark trace as for the light trace. (The trajectories corresponding to the two different gains are qualitatively similar; (*a*) actually corresponds to the lower value of μ.) (*c*) The cost function $\Gamma(t)$ given by (2.12), plotted as a function of time, for 1/200th of the time-interval of (*b*). The two traces correspond to different values of gain μ: the value of μ is three times as large for the dark trace as for the light trace. Because similar initial conditions were used, the expanded time-scale plot of $\Gamma(t)$ corresponding to figure 3 is very similar. (The time axes for (*b*) and (*c*) differ by a factor of 200, which is why the initial transient cannot be seen in (*b*).)

So, to make a proper comparison we let r_o as in §3 be a length-scale for the problem and define the dimensionless gain

$$N^{\mathrm{MCPG}} = \mu r_o. \tag{5.3}$$

Thus, our MCPG law takes the form

$$u^{\mathrm{MCPG}} = N^{\mathrm{MCPG}} \frac{|\boldsymbol{r}|}{r_o} \dot{\lambda}. \tag{5.4}$$

It follows that motion camouflage uses range information to support a high gain in the initial phase of the engagement, ramping down to a lower value in the terminal phase ($|\boldsymbol{r}| \approx r_o$). In nature, this extra freedom of gain control is particularly relevant for echolocating bats (see Ghose *et al.* 2006), which have remarkable ranging ability.

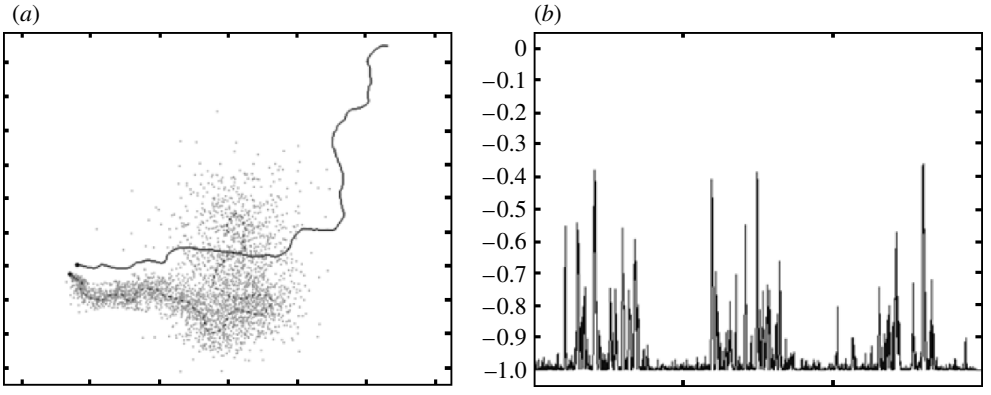

Figure 5. (*a*) Evader trajectory as in figure 4 (dashed dark line), and the corresponding pursuer trajectory (solid dark line) using control law (3.1), but with noisy measurements. $\mathbb{R}^2$-valued independent identically distributed (iid) discrete-time Gaussian noise process with zero mean and covariance matrix $\mathrm{diag}(\sigma^2, \sigma^2)$, $\sigma = 0.15|\boldsymbol{r}|$, is added to the true relative position $\boldsymbol{r}$ at each measurement instant. Similarly, $\mathbb{R}^2$-valued iid discrete-time Gaussian noise process with zero mean and covariance matrix $\mathrm{diag}(\tilde{\sigma}^2, \tilde{\sigma}^2)$, $\tilde{\sigma} = 0.15|\dot{\boldsymbol{r}}|$, is added to the true relative velocity $\dot{\boldsymbol{r}}$ at each measurement instant. These two measurement processes are then used by the pursuer to compute (3.1). The position measurements are superimposed on the true trajectory of the evader, and it can be seen that the absolute measurement error decreases as the relative distance $|\boldsymbol{r}|$ becomes small. In this simulation, the gain $\mu = 1$, the measurement interval is approximately 0.5 time units (during which a constant steering control u_{p} is applied), the pursuer moves at unit speed, and the total simulation time is approximately 1500 time units. (*b*) The corresponding cost function $\Gamma(t)$ given by (2.12), plotted as a function of time. Compared to figure 4(*b*) (light trace), there is somewhat more deviation from $\Gamma(t) = -1$, the state of motion camouflage, as a result of the measurement noise.

Analysis of the performance of the PPNG law is carried out in Ha *et al.* (1990) and Oh & Ha (1999), using arguments similar to ours (although our sufficient conditions appear to be weaker). While motion camouflage as a strategy is discussed in Shneydor (1998), under 'parallel navigation', to the best of our knowledge, the current work is the first to present and analyse a feedback law for motion camouflage.

6. Directions for further work

In work under preparation, we have generalized the analysis to the case of planar motion camouflage with respect to a fixed background object (finite point). This requires a feedback law more complicated than (3.1), since the pursuer needs to keep track of the background object in addition to the evader. We have also generalized the analysis of motion camouflage (with respect to a point at infinity) to the three-dimensional setting (Reddy *et al.* 2006). The three-dimensional analysis is made possible by the use of natural Frenet frames, analogously to the three-dimensional unit-speed particle interaction laws described in Justh & Krishnaprasad (2005).

Because we are able to treat the motion-camouflage problem within the same framework as our earlier formation control and obstacle-avoidance work (Justh & Krishnaprasad 2002, 2003, 2005; Zhang *et al.* 2004), we would like to understand how teams of vehicles can make use of motion camouflage, and whether we can

determine the convergence behaviour of such systems. Various biologically inspired scenarios for motion camouflage with teams have been described in Anderson & McOwan (2003*b*). Considering additional military applications without biological analogues, there are thus a variety of team motion-camouflage problems to study.

The authors would like to thank M. V. Srinivasan of the Research School of Biological Sciences at the Australian National University for valuable discussions and helpful comments on an earlier draft of this paper. This research was supported in part by the Naval Research Laboratory under grant nos. N00173-02-1G002, N00173-03-1G001, N00173-03-1G019 and N00173-04-1G014; by the Air Force Office of Scientific Research under AFOSR grant nos. F49620-01-0415 and FA95500410130; by the Army Research Office under ODDR&E MURI01 Program grant no. DAAD19-01-1-0465 to the Center for Communicating Networked Control Systems (through Boston University); and by NIH-NIBIB grant 1 R01 EB004750-01, as part of the NSF/NIH Collaborative Research in Computational Neuroscience Program.

References

Anderson, A. J. & McOwan, P. W. 2003*a* Model of a predatory stealth behavior camouflaging motion. *Proc. R. Soc. B* **270(1514)**, 489–495. (doi:10.1098/rspb.2002.2259)

Anderson, A. J. & McOwan, P. W. 2003*b* Motion camouflage team tactics. *Evolvability & Interaction Symposium*. See http://www.dcs.qmul.ac.uk/∼aja/TEAM_MC/team_mot_cam.html.

Collett, T. S. & Land, M. F. 1975 Visual control of flight behaviour in the hoverfly, *Syritta pipiens*. *J. Comp. Physiol.* **99**, 1–66. (doi:10.1007/BF01464710)

Ghose, K., Horiuchi, T., Krishnaprasad, P. S. & Moss, C. 2006 Echolocating bats use a nearly time-optimal strategy to intercept prey. *PLoS Biol.* **4**, 865–873, e108. (doi:10.1371/journal.pbio.0040108)

Glendinning, P. 2004 The mathematics of motion camouflage. *Proc. R. Soc. B* **271**, 477–481. (doi:10.1098/rspb.2003.2622)

Ha, I. J., Hur, J. H., Ko, M. S. & Song, T. L. 1990 Performance analysis of PNG laws for randomly maneuvering targets. *IEEE Trans. Aerospace Electr. Syst.* **26**, 713–721. (doi:10.1109/7.102706)

Justh, E. W. & Krishnaprasad, P. S. 2002 A simple control law for UAV formation flying. Institute for Systems Research Technical Report TR 2002-38. See http://www.isr.umd.edu.

Justh, E. W. & Krishnaprasad, P. S. 2003 Steering laws and continuum models for planar formations. In *Proc. 42nd IEEE Conf. Decision and Control*, pp. 3609–3614.

Justh, E. W. & Krishnaprasad, P. S. 2004 Equilibria and steering laws for planar formations. *Syst. Control Lett.* **51**, 25–38. (doi:10.1016/j.sysconle.2003.10.004)

Justh, E. W. & Krishnaprasad, P. S. 2005 Natural frames and interacting particles in three dimensions. In *Proc. 44th IEEE Conf. Decision and Control*, pp. 2841–2846 (see also arXiv:math.OC/0503390v1)

Mizutani, A., Chahl, J. S. & Srinivasan, M. V. 2003 Motion camouflage in dragonflies. *Nature* **423**, 604. (doi:10.1038/423604a)

Oh, J. H. & Ha, I. J. 1999 Capturability of the 3-dimensional pure PNG law. *IEEE Trans. Aerospace Electr. Syst.* **35**, 491–503. (doi:10.1109/7.766931)

Reddy, P. V., Justh, E. W. & Krishnaprasad, P. S. 2006 Motion camouflage in three dimensions. Preprint (arXiv:math.OC/0603176v1).

Shneydor, N. A. 1998 *Missile guidance and pursuit*. Chichester, UK: Horwood.

Srinivasan, M. V. & Davey, M. 1995 Strategies for active camouflage of motion. *Proc. R. Soc. B* **259**, 19–25.

Srinivasan, M. V. & Zhang, S. 2004 Visual motor computations in insects. *Annu. Rev. Neurosci.* **27**, 679–696. (doi:10.1146/annurev.neuro.27.070203.144343)

Zhang, F., Justh, E. W. & Krishnaprasad, P. S. 2004 Boundary following using gyroscopic control. In *Proc. 43rd IEEE Conf. Decision and Control*, pp. 5204–5209.